# NGAO TT and TTFA Wavefront Sensor Preliminary Design

KECK ADAPTIVE OPTICS NOTE XXX

Version 1.0

March 30, 2010

J. Kent Wallace, Randall Bartos, and Gautam Vasisht, JPL

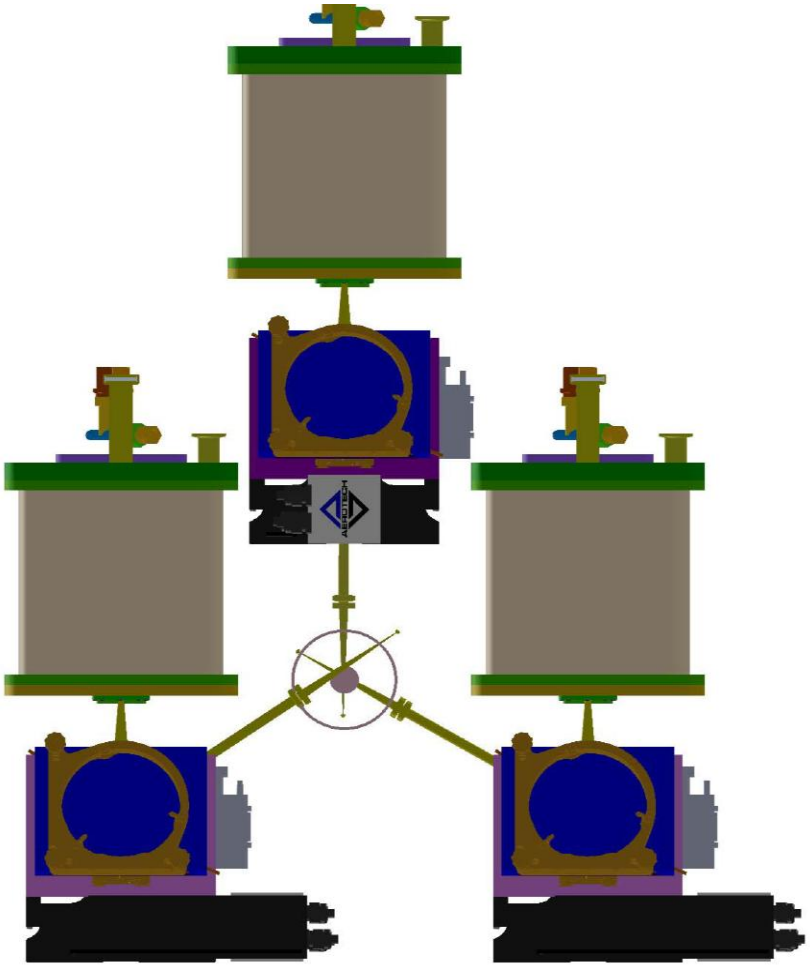

# Table of Contents

# 1. Introduction

## 1.1 Scope

This document describes the preliminary design of the low-order tip/tilt and tip/tilt/focus/astigmatism sensors for Keck's Next Generation Adaptive Optics (NGAO) system. Version 1 of this document concentrates the optical and mechanical preliminary design, and the design of the cryostat for the IR detector. It does not cover design of the object selection mechanisms, the details of the IR detector technology, reliability, or prototyping.

## 1.2 Significant Design Changes

We have detailed the optical design from the pick-off optics of the object selection mechanisms to the final focal plane. We have included rudimentary mounting for the 32x32 DM from Boston Micro Machines. Given that much of this design revolves around packaging, and most of the packaging revolves around the cryostat design, we have taken steps to detail this critical element as much as possible.

## 1.3 Reference Document

# 2. Requirements

## 2.1 System Level Requirements

## 2.2 Functional Performance Requirements: Key ones

Plate Scale: 50 mas
Zenith Angle: 30 degree at full performance, 70 degree at reduced performance
Wavelength Range: J + H band
Throughput:
Patrol Arm FOV: 5 arc sec (diameter)
Patrol Range:
    Outer Field Radius: 60 arc sec
Non-common path wavefront quality: 15 nm, rms
Wavefront calibration
Required Translation Range: +/- 10 mm
DM Pupil Size: 9.3 mm
DM/P&S WFS Registration:
Cold Room Temperature: -20 C

## 2.3 Configuration Requirements

## 2.4 Mass and Power

# 3. Overview

Our approach we starting the design of the low-order wavefront sensor (LOWFS) was as follows. We first wanted to take full advantage of all the design work that had

been done on the object selection mechanisms for the group working on the laser guide star (LGS) wavefront sensor. We recognized that there were several advantages to this approach. Not only would it save valuable design time but having common elements also makes the test and integration easier. Now, this means that we assume that the OSM's for the LGS completely satisfy their requirement both in the positioning of the theta/phi arms but also in the requirements for the tip/tilt mechanism that is an integral part of the OSM assembly. If this is the case, then the only modification we make to this design is in the re-collimation optic in the pick-off arm, in order to make it work well over the LOWFS wavelength range.

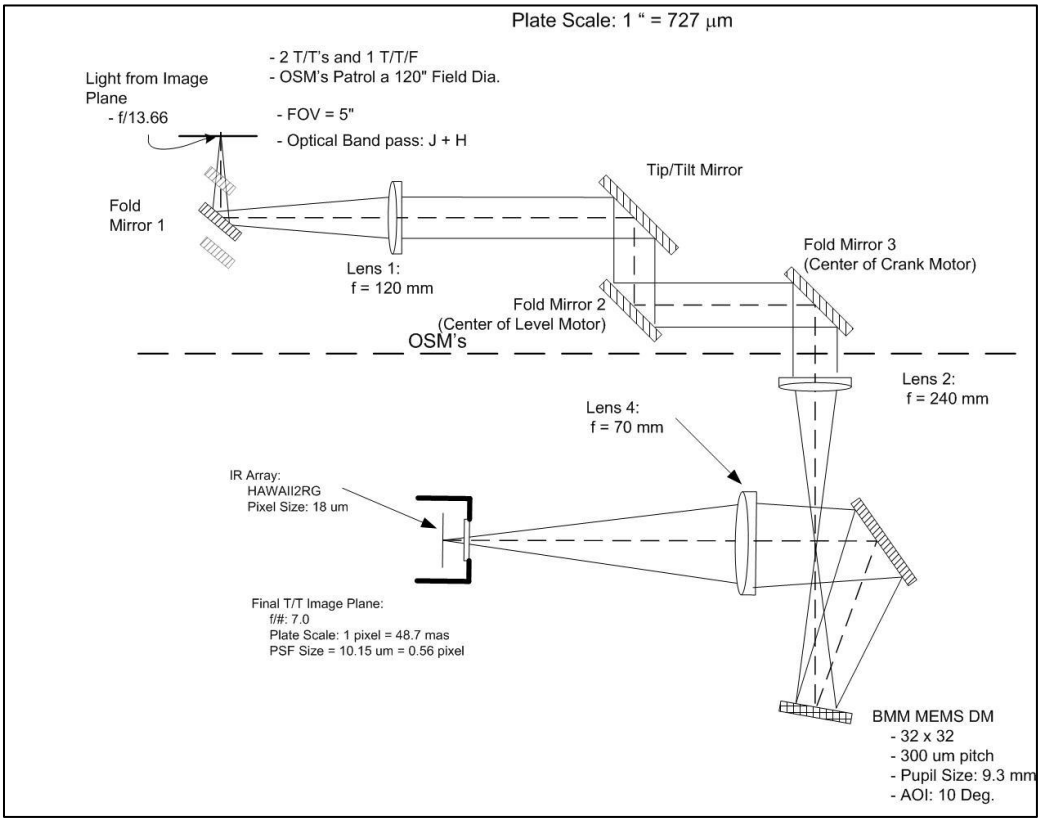


**Figure 1. Cartoon of the Keck NGAO LOWFS optical system. The elements above the dashed, horizontal line are for the object selection mechanisms. Our design philosophy was to simply inherit these from the work done on the LGS WFS (with the exception of the design for the first re-collimation optic). The work below the line is specifically for the LOWFS tip/tilt (T/T) and tip/tilt/focus/astigmatism (T/T/F/A).**

For the LOWFS design itself, the cryostat was the biggest unknown and therefore we worked on it's design in parallel with the optics design. The unknowns of the LOWFS cryostat were many: size, access, maintenance, cryo-cooling implementation, mass, performance and packaging. Therefore, the majority of the LOWFS mechanical work is really a reflection of the details of the cryostat itself, and we feel this is well understood at this point. However, there are still large details to be worked out: the mounting of the MEMS deformable mirror and packing with the rest of the system. The first is not fundamentally challenging, it's just that there are lots of details, specifications,

packaging and handling issues to be worked out for this one device. The LOWFS packaging with the rest of the instrument is under a state of constant flux. It is our goal to nail the interface of the LOWFS to the second stage relay as soon as possible.

A cartoon showing the significant components of the LOWFS relay are shown in Fig. 1. We cartoon captures the major functional elements of the design.

## 4. TT and TTFA fore-optics

### 4.1 Object Selection Mechanisms

The object selection mechanisms we take whole-sale from the effort already devoted to their design for the LGS system. We assume that the vetting of these mechanisms is sufficient to allow them to be completely adopted by the LOWFS cameras. Not only does this save significant design work up front, but it also will save significant work in the hardware integration and test phase. So we accept these items as they have been designed, including the tip/tilt mirror mechanism. The only element that is changed in our design is the re-collimation optic. It has been designed for broadband operation in the near IR. A diagram of the object selection mechanism is shown below in Figure 1. A description of this design is given in the following paragraphs.

The selection mechanism is composed of rotation stages with an offset between them. At the center each stage is a mirror, and the two mirrors together then form a periscope. This is known as a theta-phi pickoff arrangement. The ‘upper’ rotation stage, the one closest to the pick-off mirror is known as the lever motor and the ‘bottom’ stage is known as the crank motor.

The crank arm and the lever arms are balanced about their axis of rotation to prevent torque on the motor at any position of the armThe crank and lever motors use PI’s M037 and M-038 drives. All M-037 rotation stages are equipped with ultra-precise worm gear drives allowing unlimited rotation in either direction. Model M- 037.DG is a closed-loop DC motor with shaft-mounted position encoders and precision gearheads providing 3.5 µrad at a design resolution of 0.6 µrad. Model M-038.DG1 is equipped with a closed-loop DC motor with shaft-mounted position encoder and precision gearhead providing minimum incremental motion of 3.5 µrad at a design resolution of 0.6 µrad.

The tip/tilt mirror is momentum compensated mirror from Left-hand design. It is mounted in the mechanical system that is attached to the lever motor, and contains the pick-off arm.

A Honeywell 8LS125 micro-switch and a custom contour milled track serve the purpose of a fail-safe system to prevent collision of the pick-off arms with its surrounding in case of software failure.

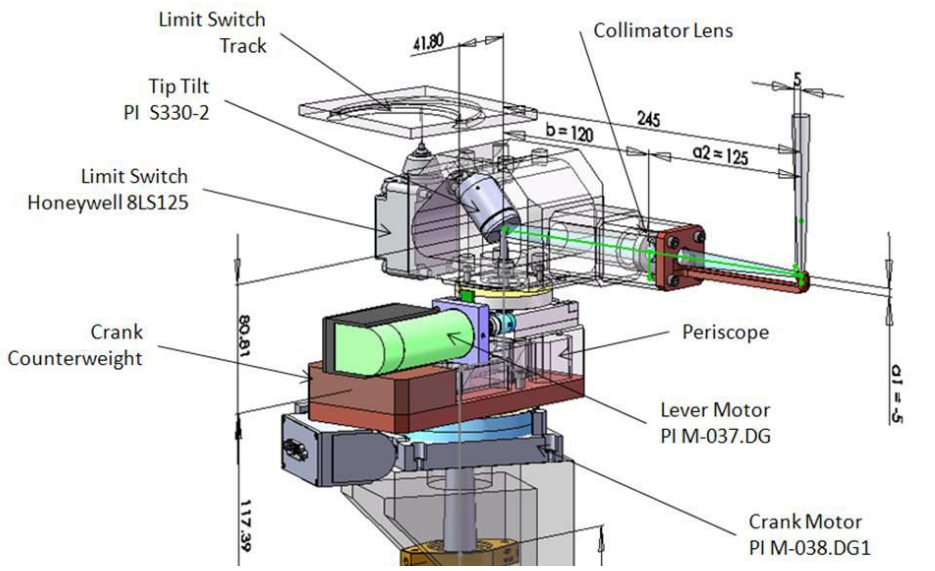


**Figure 1. The object selection mechanism. This mechanism is inherited from the design work done for the LGS WFS. It is a theta-phi design implemented with two rotation stages, one off-set with respect to the other. The upper stage is the lever, the lower stage is the crank. A contact encoder and custom limit switch track are used to prevent mechanical interference in case of software failures.**

### 4.2 Design of re-collimation Optic

This element serves two purposes. It re-collimates the beams that are picked-off in the LOWFS image plane. The beam is collimated so that the beam size is well maintained as it snake through the opto-mechanics of the object selection mechanisms. In collimating the beam, it also forms an image of the system pupil at the tip/tilt mechanism.

This optic is an air spaced achromat. The surfaces are spherical , the glasses, Fused Silica Magnesium Fluoride are readily available in high quality. Their properties are well understood. There is nothing particularly challenging about this element with regards to fabrication.

We first show an image of the object selection mechanism relay, then we show an image of the lens itself. Finally, the imaging performance is shown.

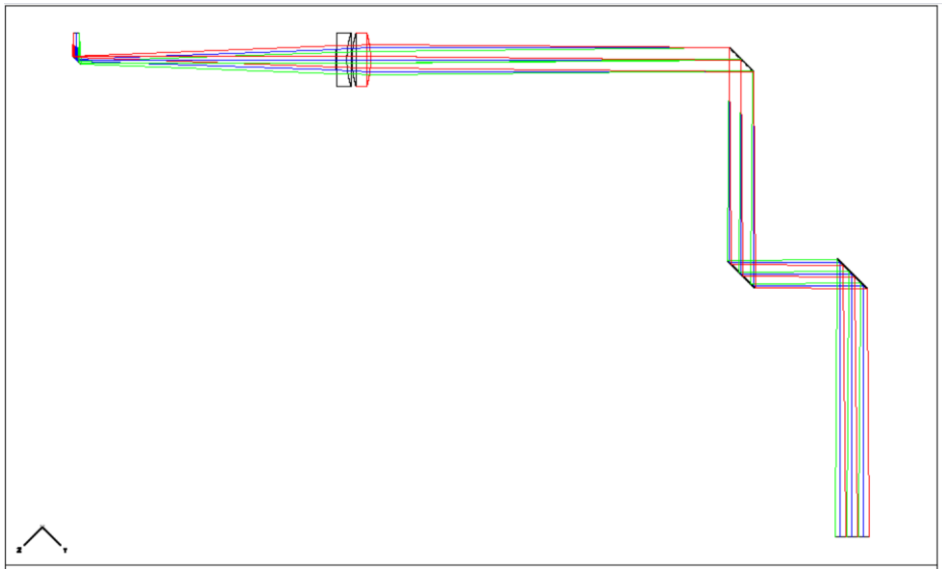

**Figure 2. The object selection mechanism optical beam path. The first element in the system is a fold mirror. The three arms of the OSM are staggered in the focal plane to avoid mechanical interference. The re-collimation optic is subsequent to this initial fold. It is an air-spaced achromat that works over J/H bands. The next optics in the beam path are: 1) the tip/tilt mirror, 2) the mirror at the center of the lever stage and 3) the mirror at the center of the crank stage.**

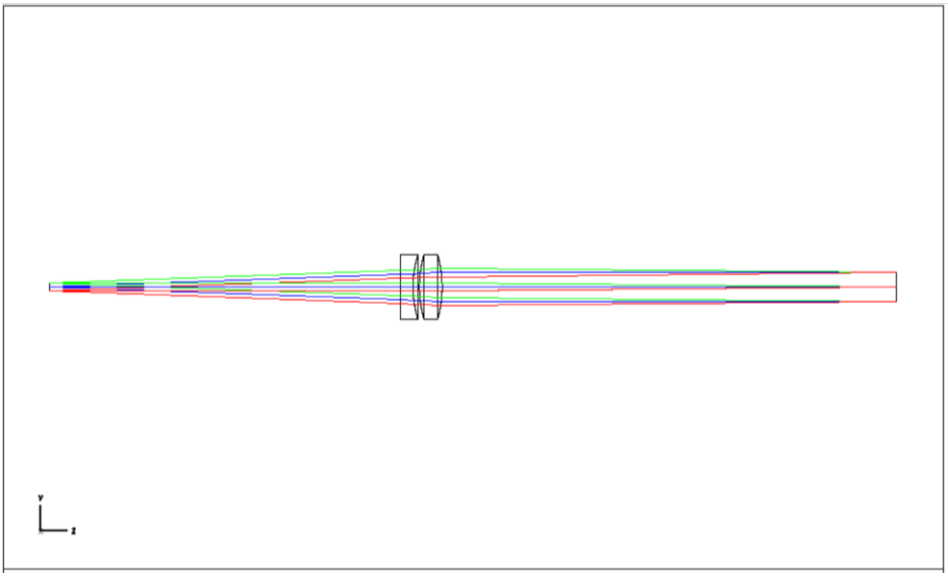

**Figure 3. The object selection mechanism re-collimation optic. The input is shown on the left, and the location of the re-image pupil is shown on the right. The field-of-view of this system is five arc seconds in diameter, on the sky.**

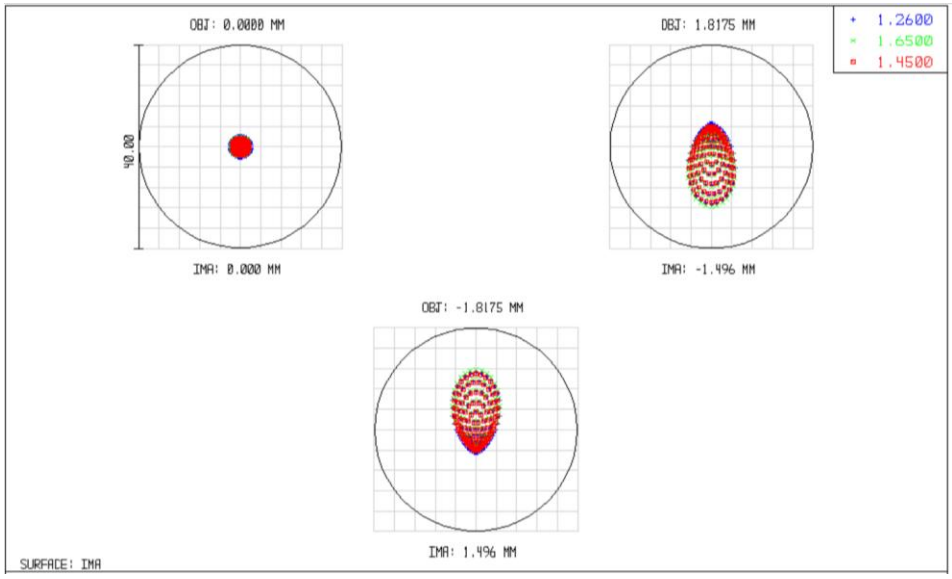


**Figure 4. This spot diagram shows the optical performance of the OSM –recollimation optic over the +/- 2.5 arcsec (on the sky) radius FOV over the required bandpass. This system is diffraction limited over this field of view.**

## 5. TT WFS Optical Design

After the optics for the object selection mechanism, we come to the optical relay for the tip/tilt sensor. There are two lenses, and these optics serve the role of: 1) relaying the system pupil to the deformable mirror and 2) relaying the intermediate focus to the final image plane at the correct plate scale. So, we'll describe each of these elements in the next sections.

### 5.1 TT Pupil Plane Imaging

This optic reimages the pupil that is at the tip/tilt mirror to the 32x32 deformable mirror. This optic also forms an intermediate focus. The focal length of this lens is about 120 mm. The imaging is roughly 1:1. Again this lens is made from Fused Silica and Magnesium Fluoride elements with spherical surfaces.

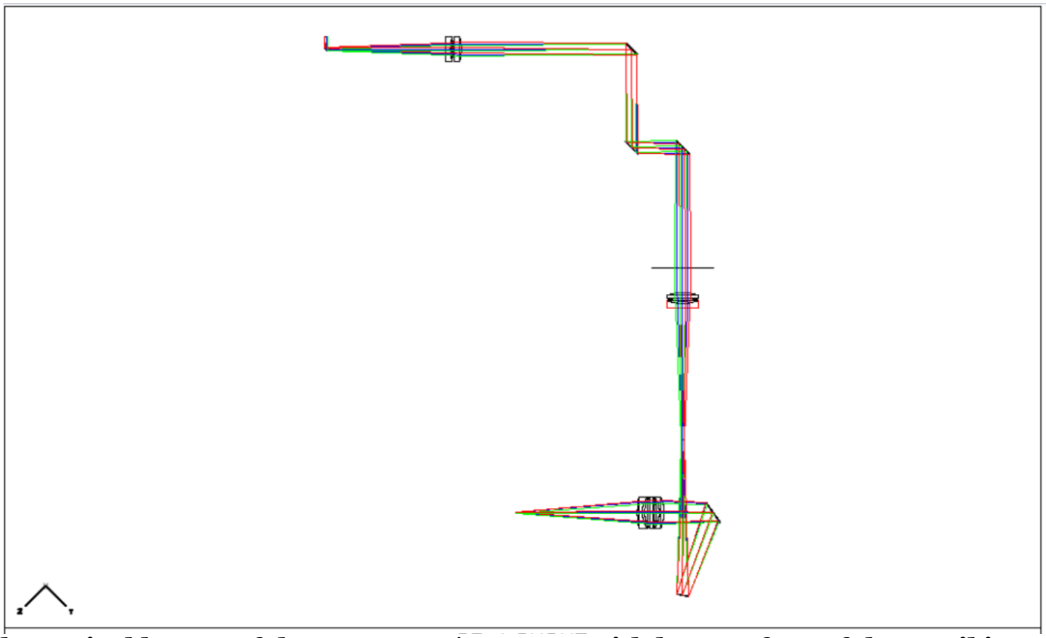

**Figure 5. The optical layout of the LOWFS T/T system with last surface of the pupil imaging lens highlighted in red. This optic re-images the pupil at the tip/tilt mirror to the BMM 32x32 DM located at the bottom of the image. This optic also forms an intermediate focus between the lens and the DM.**

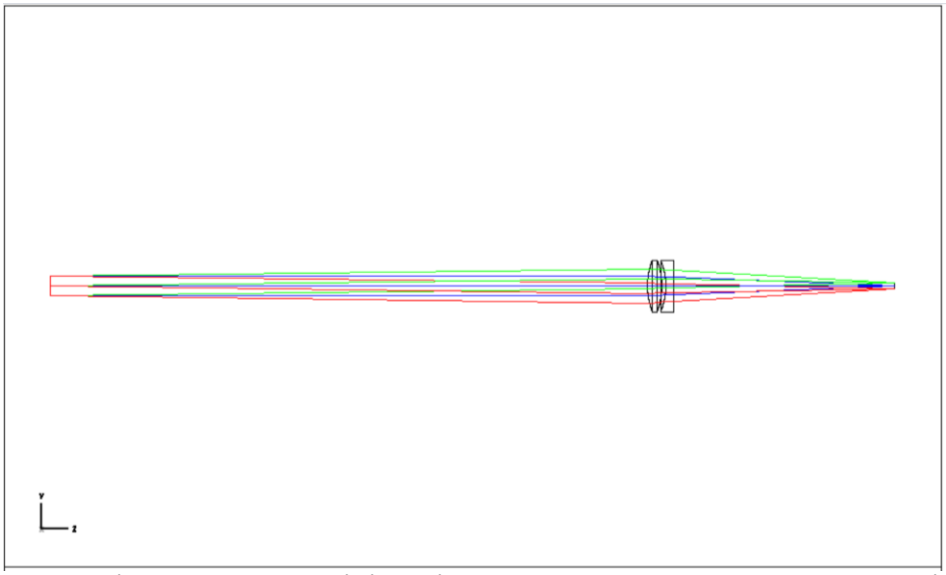

**Figure 6. An unfolded image of the pupil imaging lens. The focal length of the lens is about 120 mm, and the pupil imaging is therefore a 2f imaging system with a unit magnification.**

### 5.2 TT Focal Plane Imaging

The remaining powered optical element in this beam path is the relay lens. This element does nothing more than relay the intermediate focus formed by the pupil

imaging lens to the detector image plane with a slight change in magnification to establish the correct plate scale. The lens is again made of Fused Silica and Magnesium Fluoride, like the other lenses. Surfaces are spherical.

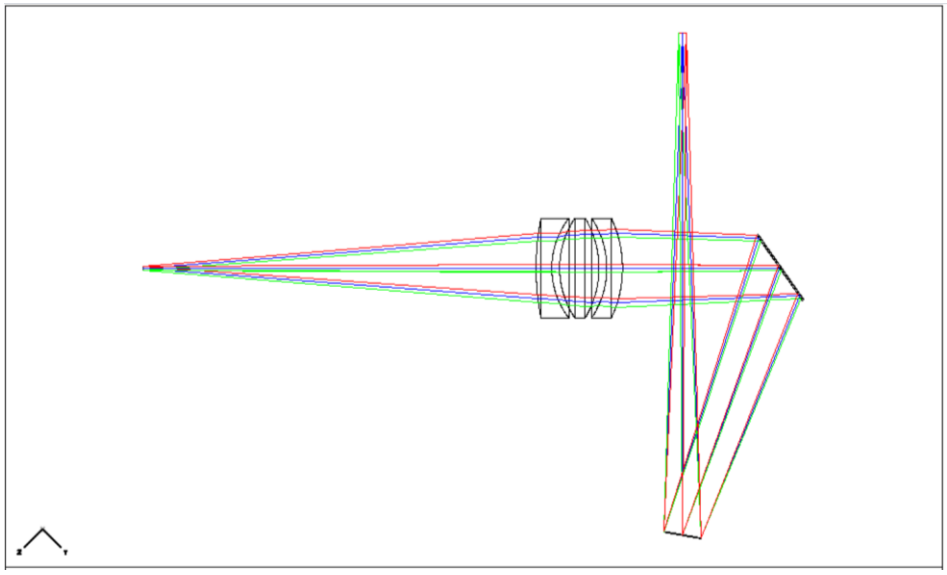

**Figure 7. This spot diagram shows the optical performance of the OSM –recollimation optic over the +/- 2.5 arcsec (on the sky) radius FOV over the required bandpass. This system is diffraction limited over this field of view.**

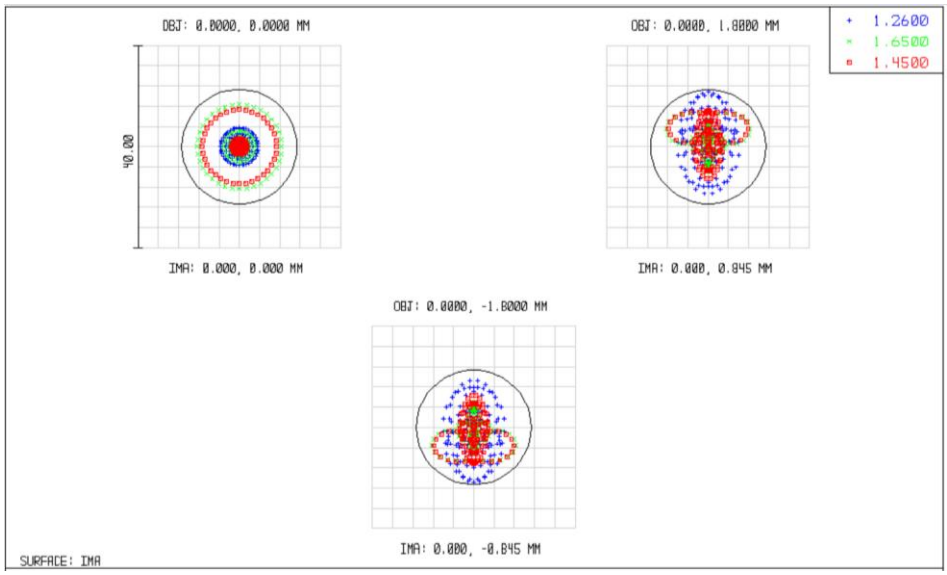


**Figure 8. This spot diagram shows the optical performance of the LOWFS System over the +/- 2.5 arcsec (on the sky) radius FOV over the required bandpass. This system is diffraction limited over this field of view.**

## 5.3 Photometry/Emissivity

## 6. TTFA WFS Optical Design

The optical design for the TTFA arm of the LOWFS inherits all of the optics previously described for the TT assemblies. Where the TT assemblies end, we add two additional optics. The first optic is a re-collimation that creates a real image of the pupil, and the second optic is a lenslet array that is placed in this pupil plane to form the 2x2 Shack-Hartman spots on the final detector.

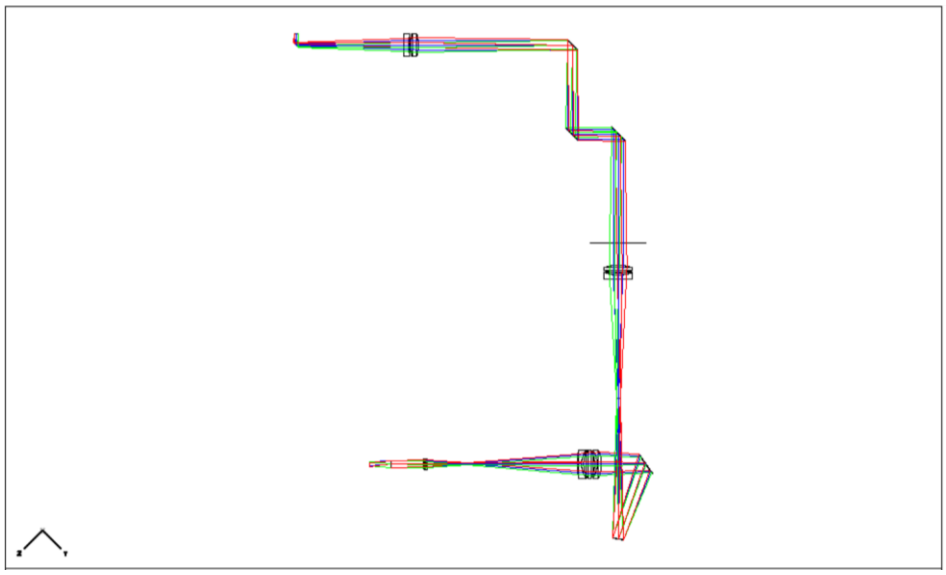

**Figure 9. Complete optical path of the TTFA arm of the LOWFS. The optics are completely common to the TT assembly with the exception of the last two elements: 1) the re-collimation achromat and 2) the lenslet array.**

### 6.1 Recollimation Lens and Lenslet

The TTFA re-collimation lens and the lenslet are show below in Figure 10. The optical layout shows the beam path from the intermediate focus before the DM to the fold mirror, relay lens, and then the re-collimation optic and the lenslet. The recollimation lens has a focal length of about 40 mm and creates a real image of the pupil about 30 mm after the last surface of the lens assembly. The lens itself is very similar to the other lenses in the system: the two glasses are Fused Silica and Magnesium Fluoride, and all the surfaces are spherical. It is an air spaced achromat.

The lenslet is shown as a paraxial lens at the moment. A custom lenslet is likely in order for this element. As shown, the sub-aperture are about 3.2 mm square in a 6.4 mm diameter pupil. The focal length is 20 mm and this then gives a plate scale of roughly 50 mas per pixel on the final image plane. The four spots are separated from each other by roughly 180 pixels in the x and y direction on the array.

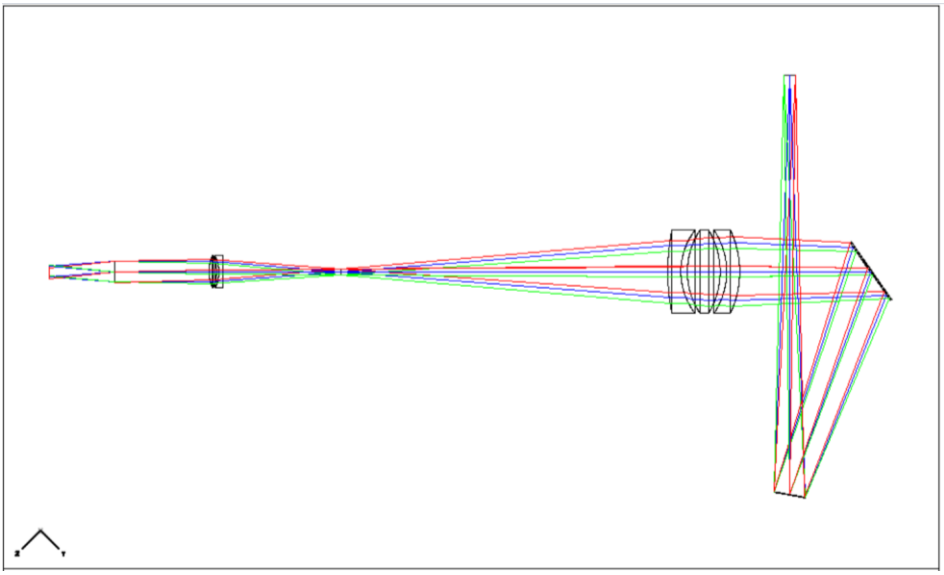

**Figure 10. A closer view of the last section of the optical beam path. This optical layout starts at the intermediate focal plane of the pupil imaging lens, and the ends at the focal plane of the detector. The re-collimation optic is about 10 mm in diameter and has a focal length of about 40 mm. The real pupil is formed about 30 mm after the last surface. The lenslet array divides this pupil into 2x2 sub-apertures.**

### 6.2 Photometry/Emmisivity

## 7. Opto-mech design

The opto-mechanics for the LOWFS is shown below in Figure 10. We have placed all the key elements on a single translation stage that will accommodate any changes in the LOWFS focal plane position. The stage also contains the object selection mechanisms on the entrance to the optical system. This design is compact to aid in packaging and ensure instrument stability. All the rest of the elements will be mounted with off-the-shelf components. The only exception is the deformable mirror which will need some significant design time. The cryostat will also be supported directly off of the translation stage.

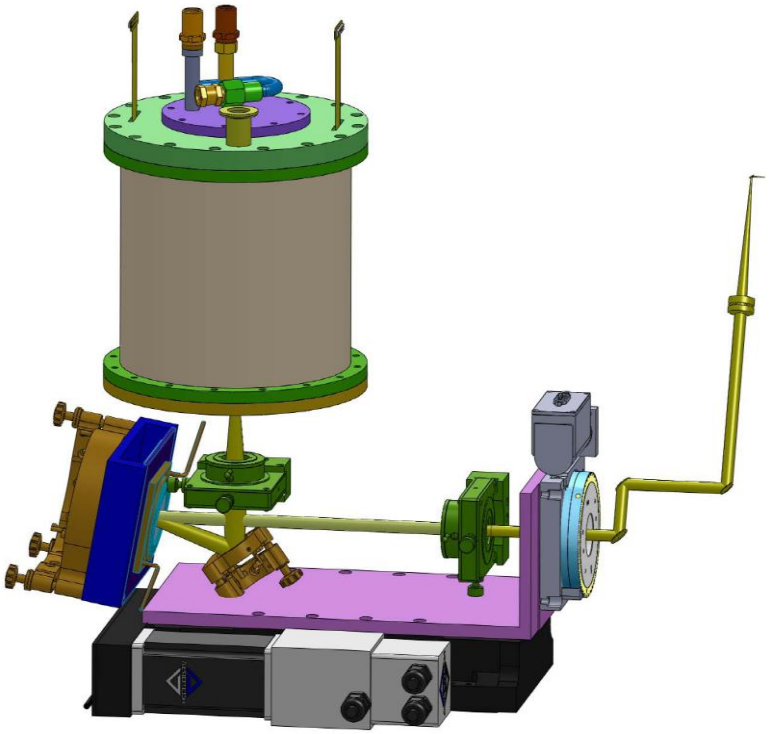

**Figure 10. The packaging for the LOWFS TT arm. All opto-mech components will be supported on a single translation stage. The mounts for the pupil imaging lens, fold mirror and relay mirror can be handily accomplished with off-the-shelf components. The mounting of the DM will require careful thought and some custom design.**

### 7.1 OSM Lens mount

This custom doublet, like all the custom elements, will be delivered in a custom lens cell. This cell will then be mounted into the pick-off arm of the object selection mechanism. Given this modular approach, we foresee no difficulties as long as the interface between the two components are well defined.

### 7.2 Relay Lens Mount

The relay lens, also a custom lens in its own cell, will be mounted in an off-the-shelf directly to the interface plate to the translation stage. This stage will have x, y, and z translational degrees of freedom to aid in the alignment.

### 7.3 DM Mounting

The mounting of the 32x32 BMM DM will require significant design work. It needs to not only provide stable mounting of the DM itself, but also accommodate the multitude of cables as well. There is the possibility that the face sheet will also need to be evacuated to keep the humidity low. Currently, we have simply adopted the same

mounting method as used by the DM in the second-stage relay. This placeholder does a fair job of capturing the size of the final DM mount.

### 7.4 Cryostat Lens mounts

The cryostat lens will be mounted directly to the cryostat itself. The custom triplet will have its own lens cell. We envision a threaded lens tube attached directly to the cryostat front face. The threading will allow fine adjustment of the custom lens in the longitudinal direction relative to the focal plane.

### 7.5 Translation Stage

All these mechanics will be mounted to an Aerotech translation stage. These stages are driven by a worm gear to provide bi-directional positioning repeatability. These stages can carry heavy loads and maintain position resolution at the micron level. The stages can also have motors mounted on either side of the rails as well as the back to improve instrument packaging.

## 8. Cryostat Design

The opto-mechanics for the LOWFS is shown below in Figure 9. We have placed all the key elements on a single translation stage that will accommodate any changes in the LOWFS focal plane position. The stage also contains the object selection mechanisms on the entrance to the optical system. This design is compact to aid in packaging and ensure instrument stability. All the rest of the elements will be mounted with off-the-shelf components. The only exception is the deformable mirror which will need some significant design time. The cryostat will also be supported directly off of the translation stage.

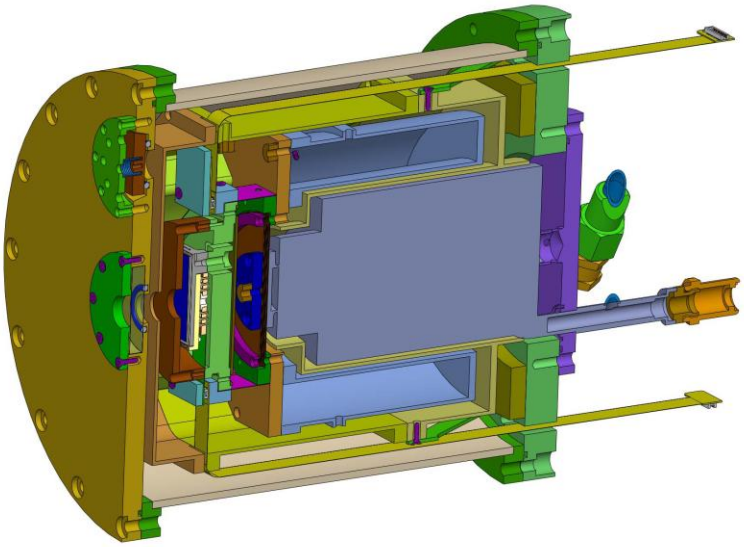

**Figure 11. LOWFS Cryostat. The outer flanges are eight inches in diameter and the chamber itself is 7 inches in diameter. The cryocooler is a CryoTiger mixed gas Joule-Thompson cooler. All the electronics are mounted externally (not shown).**

### 8.1 Array Mount

The HAWAII2RG array from Teledyne comes with two mounting options – four legs or three legs. The three leg array mounting design (shown in Figure 12) is more properly constrained and we choose this method. This array mount is then mated to the detector cold plate via three linear flexures. This flexure design minimizes the transmission of mechanical stress to the array mounting frame. The details of these flexures is shown below in Figure 11.

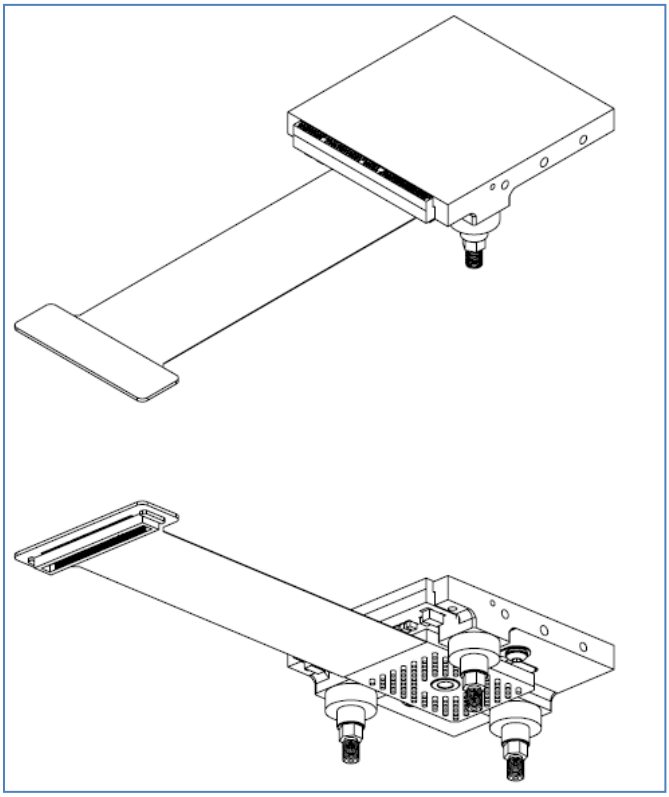

**Figure 12. Mechnics for the array mounting. The three legged option (shown above) allows for a more kinematic and mechanically stable form of mounting. The flex cable coming from the array and leading to a Hirose connector contains all the electrical signals to and from the array.**

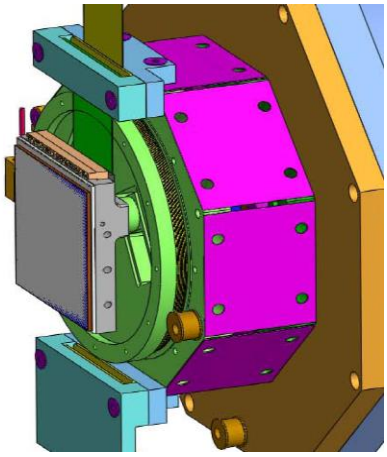

**Figure 13. The mounting of the array legs to the cryostat is via three linear blade flexures (shown as the green circular disk above). This method of mounting minimizes the transmission of unbalanced forces through the legs to the array.**

## 8.2 Cryo-cooler choice

We have selected the CryoTiger for our means of cryo-cooling. The CryoTiger is very simple to operate, provides sufficient steady-state cooling power for our small cryostat (shown in Figure 15 below). The cooler also imparts very little vibration as compared to other cryocooling options as shown in Figure 16 below. The lines for the compressed gas can be quite long, and empirical evidence is that the cooling becomes more efficient the longer the lines get. Therefore, the compressor can be quite distant from the cryostats. They can also be mounted separately to aid in the isolation of the mechanical noise from the compressors.


**Figure 14. Compressor and cold head for the Cryo-Tiger mixed-gas Joule-Thomson cooler. The mixed gas lines can be quite long.**

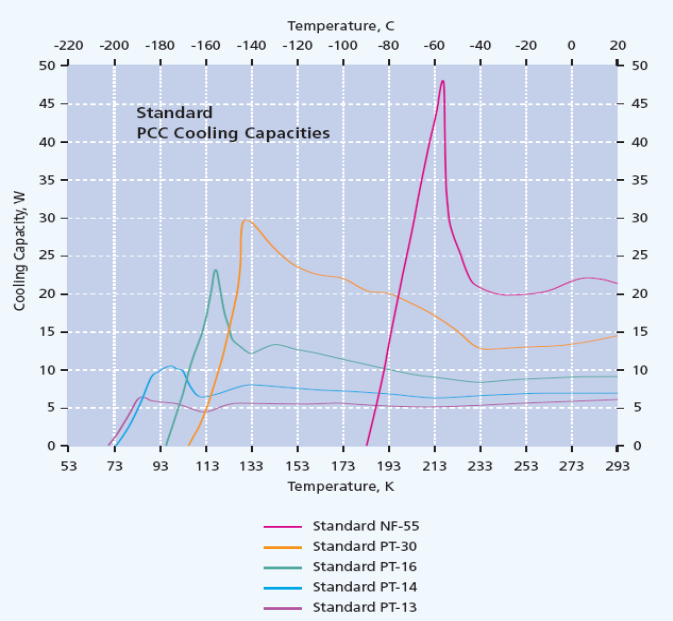


**Figure 15. Cooling capacity for different models of cryocoolers. We plan on using the Standard PT-14. This has several Watts of margin at 90K.**

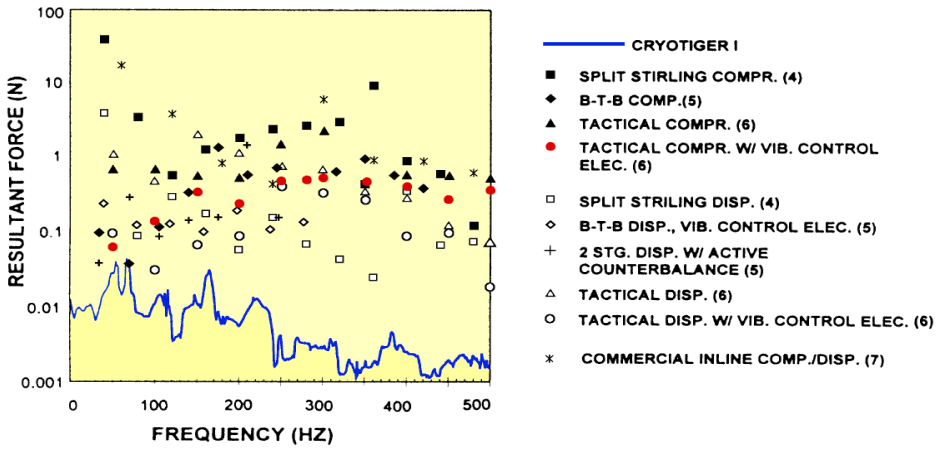


**Figure 16. Power spectrum of the vibrations for the CryoTiger in comparison to other cryocooling options. The blue line is the cryotiger, its level of vibration is several orders of magnitude lower than other options because of its very simple operation.**

## 8.3 Getters

There are two types of getters in the cryostat: Zeolite and charcoal. The charcoal getter is immediately surrounding the cryotiger cryocooler. The Zeolite is kept in an area towards the front of the cryostat where the temperature is warmer.

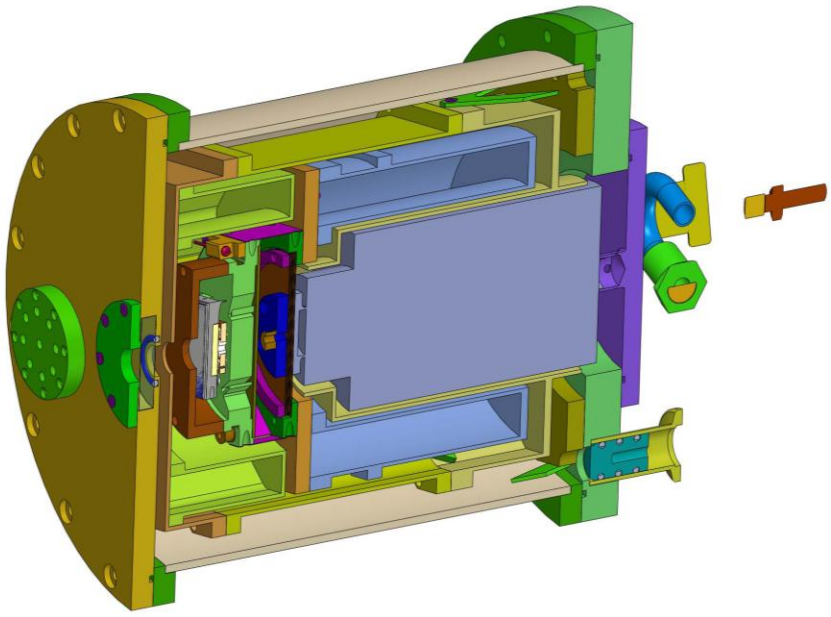

**Figure 17. There are two getter volumes in the cryostat. The blue shell around the central cryostat holds the charcoal getter. The light green volume surrounding the detector cover on the left holds the Zeolite.**

## 8.4 Heaters/Thermisters

## 8.5 Vacuum Port

We use a very compact vacuum port for the cryostat. The valve is placed in the back flange between the outer disk of the cryotiger and the outer bolt pattern of the back flange as shown below in Figure 18.

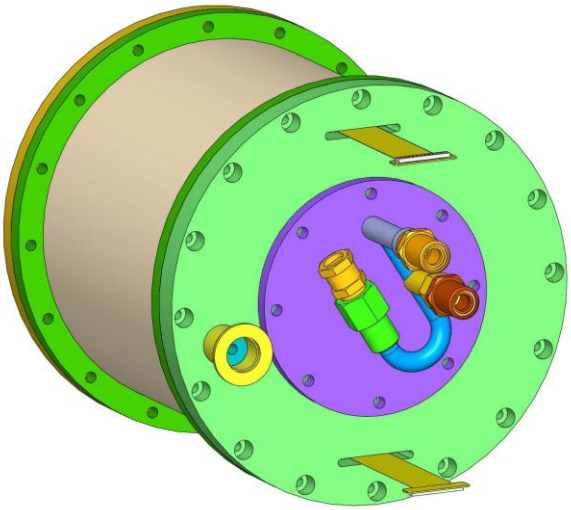

**Figure 18. The compact vacuum valve is shown as the yellow colored plug in the left side of the back flange. The plug is shown in the light blue internal to the valve.**

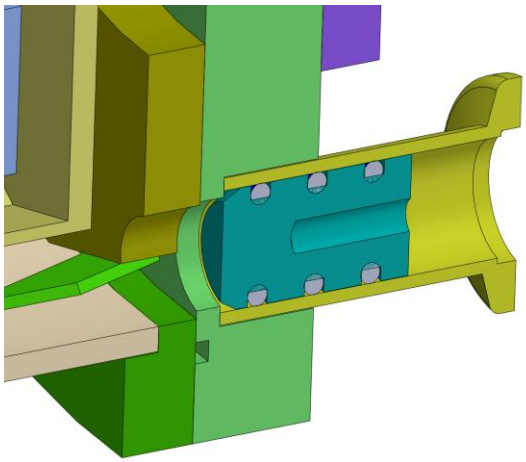

**Figure 19. Cross-section of the miniature vacuum valve. The central portion of the blue plug is threaded. With additional vacuum hardware (not shown), the plug is removed with a tool that is part of a vacuum-tight joint at the flange end.**

The operation of the vacuum valve is as follows. A special adaptor is mated to the end of the vacuum valve. This adaptor has, in a 'T' configuration both the threaded tool to remove the plug under vaccum, and the lines that lead to the vacuum pump. When the 'T' joint and vacuum lines are evacuated, the threaded tool that is integral to the joint is used mated to the plug and the plug pulled back until the cryostat has an open pathway to the vacuum line. The cryostat is then pumped down. When pressure reaches an acceptable level, the plug is re-installed, the insertion tool is un-threaded and removed, and the vacuum line can then be detached. The advantage of this design is that the vacuum hardware is greatly reduced in size.

### 8.6 Thermal Loading Calculations

We have performed the thermal loading calculates to help us determine the required cooling capacity of the cryocooler and it's steady state operational temperature. This mode is composed of two key components: the thermal conduction model and the radiation model.

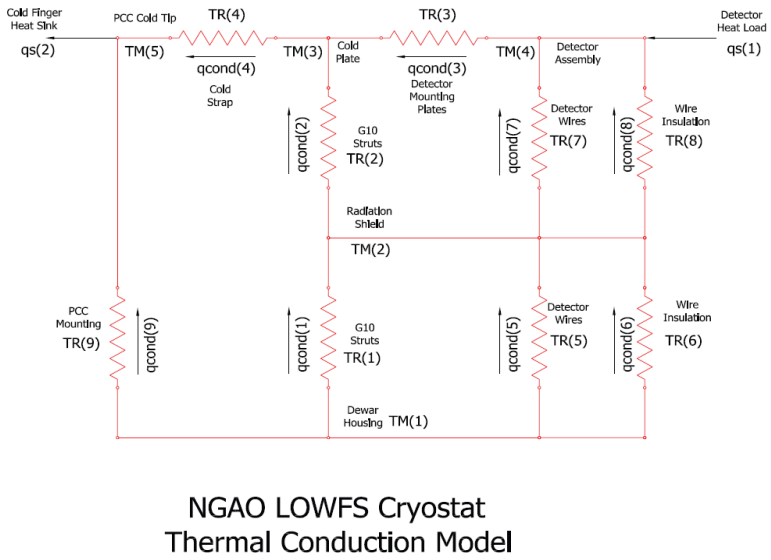


**Figure 20. The thermal conduction model for the LOWFS Cryostat.**

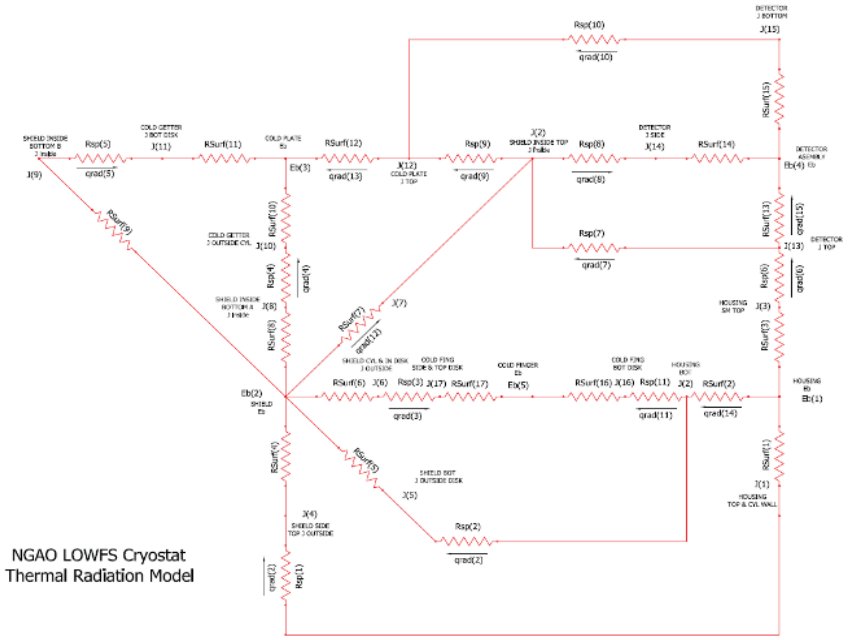


**Figure 21. Resistive model for the LOWFS cryostat.**

A preliminary thermal analysis was performed on the LOWFS cryostat. The cryostat is required to maintain the LOWFS detector array at a temperature of ~90 degrees Kelvin or less. The objectives of the analysis were as follows:

· Preliminary steady–state thermal analysis showing the temperature distribution at the end of a cool down cycle.

· Preliminary cool down analysis incorporating the cooler capacity as a function of temperature.

The model should be adequately detailed to give the cool down time with a maximum error of 50% A lumped parameter thermal model was used to perform the thermal analysis of the LOWFS dewar. The differential equations of the thermal model were solved numerically using MATLAB to produce a cool down simulation of the LOWFS dewar. The steady state performance of the dewar was obtained by looking at the final values of the cool down simulation after the dewar components had reached their steady state temperature. The LOWFS dewar cool down simulation assumed that 5 watts of cooling power was available. The thermal analyses assumed that the detector was off and not dissipating heat until the detector reached its final operating temperature below 80 degrees Kelvin. The LOWFS dewar simulation model took approximately 11 hours to reach a steady state temperature below 80 degrees Kelvin. The LOWFS dewar radiation shields reached their steady state temperature after approximately 40 hours. Once the 80 degree Kelvin detector temperature was achieved, it took the dewar simulation model approximately 1 watt of cooling power to maintain the LOWFS dewar component

temperatures at their steady state values in a 293 degree Kelvin ambient environment assuming a maximum detector heat load of 0.25 watts.

# 9. Electronics Design

## 9.1 Array Read out electronics

The array is a HAWAII2RG. It is the best low-noise, near IR detector available. Although a full science grade array is quite expensive, we plan to procure arrays that are not fully operational. We only require a small number of pixels in order to make the tip/tilt measurement. We read out the array with a set of Leach Electronics that includes boards for clocks, biases and a video card. These electronics interface to the computer via a communications card.

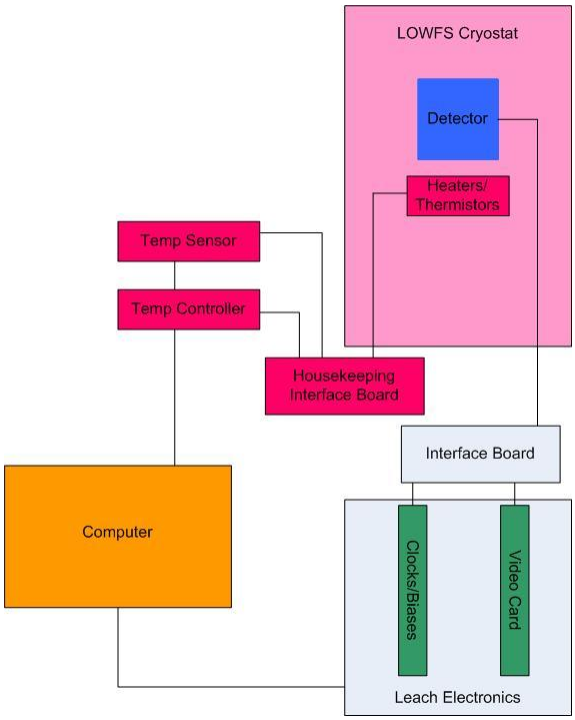


**Figure 22. Electronics diagram for the LOWFS sensor. All electronics for the array are external to the cryostat. The flex cable from the array is extended through the back cover to interface boards external to the cryostat. These interface face boards then lead to the Leach readout electronics (the clocks biases card and the video card). House keeping signals (heaters, thermistors) come from a different flex cable.**

## 9.2 Array Heaters

## 9.3 Temperature Sensors

For the temperature sensors, we will use the Cryo-Con S900-DB silicon diodes. The physical package for these sensors is small (0.3 inches in diameter) . They are mounted on a small copper puck with a through hole for a mounting screw. The

connecting wires are rather delicate, and this style of packaging lends itself to mounting the sensor with minimal risk of breaking them off. The SM package includes an insulating substrate and is designed for direct surface mounting. It can be easily attached to any flat surface. Features include extremely small size and 3” (7.6cm) copper leads that greatly simplify thermally anchoring.

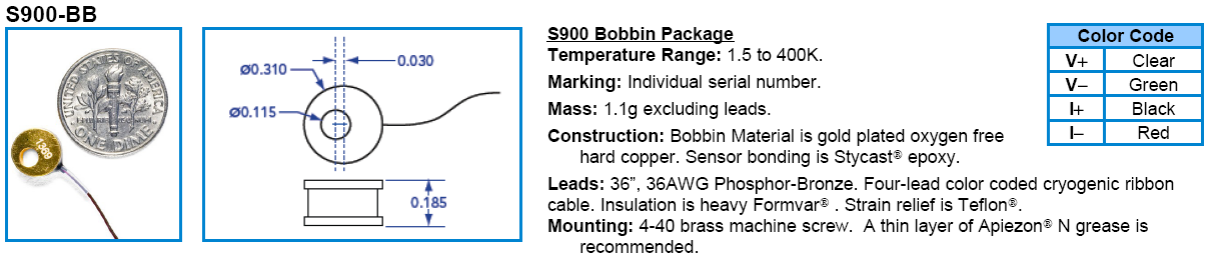


**Figure 21. Silicon diode temperature sensor for the LOWFS Cryostat. The element is quite small but the packaging lends itself to easy mounting.**

### 9.4 Temperature Monitors

For the temperature monitor, we will use the Cryo-Con Model 18, 8 channel temperature monitor.The Model 18 has eight independently multi-purpose sensor inputs. Virtually any cryogenic temperature sensor from any manufacturer can be selected by a single setting of the front panel. In addition to its high accuracy/performance and low noise design, unique features include: Internal Data Logging, Ethernet Connectivity, a large easy to read display and extensive utility software.

The front panel consists of a large, bright Vacuum Fluorescent display and a 5-key keypad. Most features and functions can be accessed via this simple and intuitive menu driven interface. All eight temperature readings are displayed in a 2 x 4 matrix.

The Model 18 connects directly to any 10/100 Base-T Ethernet Local-Area-Network or directly to any PC. Simple connection to any existing Local Area Network allows stable, precise, cost-effective measurements in laboratory or industrial environments as well as in remote, distributed data acquisition systems.


**Figure 22. The temperature monitor for the LOWFS Cryostat.**

### 9.5 Array Thermal Control

To control detector head temperature and to provide monitoring of temperatures at various points inside the dewar, we will use the Cryo-Con Model 32B, 2 sensor inputs and dual control loops.The Loop #1 Heater channel is a linear, low noise RFI filtered current source that can provide up to 1.0 Ampere into 50 Ω or 25 Ω resistive loads. Three fullscale ranges are available in decade increments. The standard Model 32 offers a 0 to 10 Volt output for a second control loop. This may be used with a programmable booster power supply where dual-loopor high power control is required.


**Figure 23. The temperature controller for the LOWFS cryostat.**

## 10. Status

### 10.1 Requirements Compliance

### 10.2 Remaining Work to do